Dent. Mater. J.
ISSN 0287-4547

DMJ

DENTAL MATERIALS JOURNAL

Volume 43,
Number
1
February 2024

AN OFFICIAL
JOURNAL OF

THE JAPANESE SOCIETY
FOR DENTAL MATERIALS
AND DEVICES

JAPAN SOCIETY FOR
ADHESIVE DENTISTRY

The Japanese Society
for Dental Materials and Devices
http://www.jsdmd.jp/en_journal/en.html

DENTAL MATERIALS JOURNAL

AN OFFICIAL JOURNAL OF
THE JAPANESE SOCIETY FOR DENTAL MATERIALS AND DEVICES
JAPAN SOCIETY FOR ADHESIVE DENTISTRY

Vol. 43, No. 1, February 2024

Contents

Dental Materials Journal 2024; 43(1): 97–105

Influence of restorative materials on the mechanical properties of maxillary first molars with different degrees of cryptic fractures and defects: A finite element analysis

Jiaying FENG[1], Mingzhu CHAI[1], Ke ZHANG[1], Jinjian LIU[1] and Xin LI[2]

[1] *Department of Oral Clinical Medicine, School of Stomatology, Jinzhou Medical University, Liaoning, China*
[2] *Shenyang Medical College, Shenyang, China*
Corresponding author, Xin LI; E-mail: httplixin@163.com

This study aimed to apply finite element analysis to evaluate the effects of pile materials with different elastic moduli and cement materials on the stress distribution between the remaining tooth tissue and cryptic fracture defects. A three-dimensional finite element model was established for 20 maxillary first molars with hidden fissures and mesial tongue-tip defects. Two levels of hidden cracks and three types of pile and adhesive materials were used in the design. The stress distribution and maximum stress peak in the remaining tooth tissue and crack defects were determined by simulating the normal bite, maximum bite, and lateral movement forces. When titanium posts, zinc phosphate binders, and porcelain crowns were used to repair the two types of deep cracked teeth, the maximum principal stress at the crack and dentin was the smallest. As the crack depth increased, the maximum principal stress of the residual dentin and crack defects increased.

Keywords: Cracked tooth syndrome, Dental materials, Elastic modulus, Finite element analysis, Post and core technique

INTRODUCTION

Cracked teeth syndrome (CTS) refers to a condition where subtle cracks are present on the surface of the tooth crowns and are difficult to detect at an early stage. Its diagnosis and treatment are difficult for clinicians owing to the variation in symptoms[1]. Frequently, untimely treatment results in the continued development of cracks, causing pulp periodontal inflammation and leading to the extraction of the affected tooth in severe cases[2]. The first molar is the first permanent tooth that erupts in the mouth; it is located in the main bearing area of the dentition. Additionally, it has the highest bite force and is the most prone to fractures[1]. The results of an epidemiological investigation revealed that CTS had become the main cause of tooth loss after caries and periodontal disease; therefore, early detection and proper treatment of cracked teeth are crucial[3].

The key to treating CTS is eliminating local stress concentrations and preventing further crack propagation. In stomatology, most structures are affected by the bite force, and finite element analysis (FEA) is an effective method for detecting the stress distribution in teeth under the action of force. Several studies have demonstrated that FEA can be applied in the field of oral prostheses[4-6]. Previous studies have compared the stress distribution of inlay and all-porcelain crown repairs for cracked teeth using FEA. Both methods can prevent further crack propagation; however, the stress at the bottom of the restoration and crack area in full-crown repair is significantly reduced[7]. This is consistent with the clinical finding that total crown therapy is the best approach to achieving the therapeutic objectives of CTS[8-10]. For damaged teeth with defects, the presence of one or more dentin wall defects in the tooth's crown after root canal therapy (RCT), post-repair, or total crown treatment can effectively reduce the failure rate of a repair treatment[11]. However, without proper design and materials for a post-core crown restoration, teeth are more likely to break. Therefore, emphasis should be placed on enhancing the flexural strength of the affected tooth before post-core crown restoration. Notably, reasonable design and material selection can enable teeth to bear a uniform bite force and reduce the generation of stress concentration areas during chewing after restoration.

Various factors, such as post-core and post-core binder materials with different elastic moduli and the stress direction and magnitude of the prosthesis, affect the stress distribution and magnitude of the residual dental tissue and prosthesis after post-core crown restoration, thereby altering the restoration effect and survival rate of affected teeth[12]. Although various repair approaches have been used to treat CTS in previous clinical trials, most treatment regimens have not been designed based on evidence. Guidelines for treating CTS have been provided; however, considerable variations exist in treating individual teeth with the same condition. According to doctors and specialists, knowing the best treatment for individuals with the same condition is impossible[13].

Therefore, this study aimed to evaluate the effect of post systems with varying elastic moduli on the stress distribution in residual dentin and cryptic crack defects to prevent tooth fracture and the further spread of cryptic cracks.

Received Jun 21, 2023: Accepted Oct 12, 2023
doi:10.4012/dmj.2023-151 JOI JST.JSTAGE/dmj/2023-151

MATERIALS AND METHODS

Imaging data of the right maxillary first molar without caries and proper periodontal health were obtained using cone-beam computed tomography to establish a geometric model of maxillary first molar fractures with defects. The selected imaging data were the maxillary first molar of a 24-year-old adult female with a total length of 19.5 mm, crown length of 7.2 mm, root length of 12.3 mm, crown proximal distal diameter of 10.3 mm, neck proximal distal diameter of 7.2 mm, crown buccal tongue diameter of 11.8 mm, and neck buccal tongue diameter of 10.8 mm. The reverse modeling software, Mimics19.0, was used to separate each part of the dental tissue according to different gray values. Geomagic software was used for analysis and refinement, thereby making the geometric model more accurate. Furthermore, the solid model was exported to the SolidWorks 2017 software. The boolean operations in Sketch were used for segmentation and combination. After RCT, the root canal component was repaired, and the gutta-percha component was separated to make it conform to the shape of the root canal. The defect structure was designed as a mesial tongue-tip defect, ranging from the buccal to the mesial sulci of the occlusal surface, distal to the lingual sulci of the occlusal facial surface, and from the gingival end to 2 mm above the cementum boundary. Cryptic cracks occurred at the junction of the mesial tongue-tip section and the distal lateral axial wall. Their direction was buccal-lingual, the width was 40–100 μm, and the depth was 1 mm (Crack 1 mm, C1) and 2 mm (Crack 2 mm, C2) under section; they developed at the side of the medullary chamber. The edge of C1 was completely wrapped by the full crown after repair, and the end of C2 was located at the root of the full crown edge (Fig. 1). After the porcelain crown preparation, the height of the preparation body was 5.1 mm, the mesio-distal diameter was 8.2 mm, and the buck-lingual diameter was 9.8 mm.

In this study, piles were repaired using the palatal root. A pile model was established based on its external dimensions. The length of the tooth inner post was 10.0 mm, and the diameter of the proximal occlusal surface was 1.5 mm, the diameter of the proximal root tip was 0.9 mm. The length of the post is two-thirds of the root length. Currently, the root canal is filled by three components: the gutta-percha, pile, and pile bonding layer. In the experiment, three types of post and binder materials were used. All materials formed a two-stage post-core structure with a resin core, which can be categorized into no-post (NP), pure titanium post (PTP), gold alloy post (GAP), and glass fiber post (GFP) based on pile material type. The binders are 3M RelyX Unicem resin binder (3M), glass ionomer (GI), and zinc phosphate (ZP). Three-dimensional models of the maxillary first molars restored with resin filling and post-core-crown restoration (Fig. 2) were obtained.

Various parameters and model assumptions were considered. Corresponding mechanical properties were assigned to each organization using ANSYS 2021 R1 software (Table 1)[14-20]. A three-dimensional mesh division was performed on each structure of the model, with a mesh size of 0.5 mm and even division

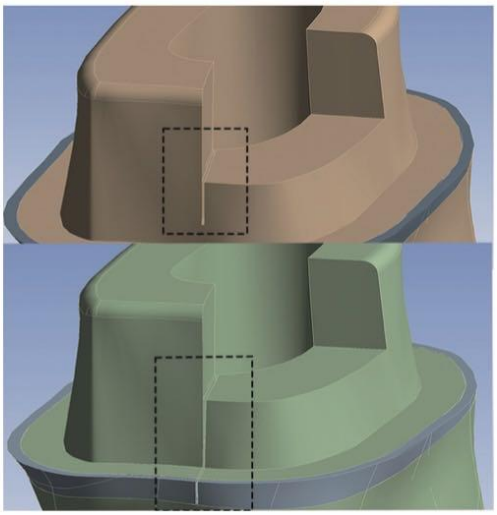

Fig. 1 Mesial tip defect preparation with a crack of 1-mm depth under section (top); Mesial tip defect preparation with a crack of 2-mm depth under section (bottom).
The dotted box indicates the crack.

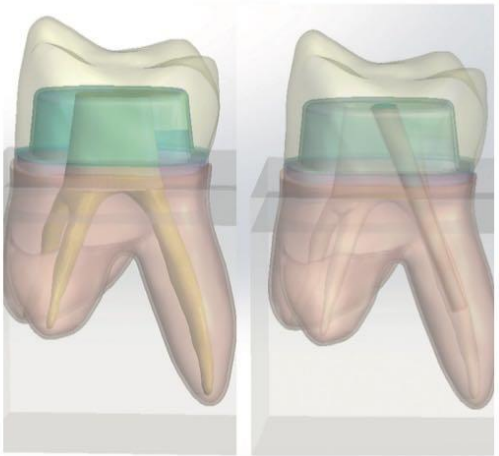

Fig. 2 Geometric modeling of maxillary first molars with cleft palate and mesial tip defects repaired by resin filling (left); Geometric modeling of maxillary first molars with a cleft palate after post and core repair (right).

Table 1 Material properties

Material	Elastic modulus (MPa)	Poisson ratio
Enamel	84,100	0.33
Dentin	18,600	0.31
Periodontal membrane	68.9	0.45
Cortical bone	13,700	0.30
Cancellous bone	1,370	0.30
Zinc phosphate binder	22,400	0.35
Glass ionic binder	4,000	0.35
3M RelyX Unicem resin binder	4,900	0.27
Zirconia all-porcelain crown	200,000	0.31
Resin nucleus	12,000	0.30
Pure titanium pile	112,000	0.33
Gold alloy pile	80,000	0.33
Glass fiber pile	40,000	0.26
Gutta-percha	141.9	0.45

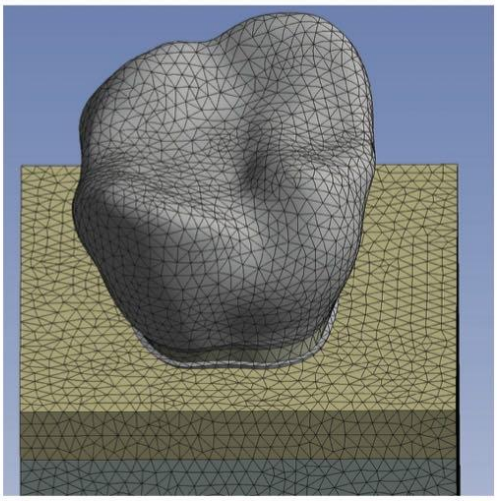

Fig. 3 3D mesh generation.

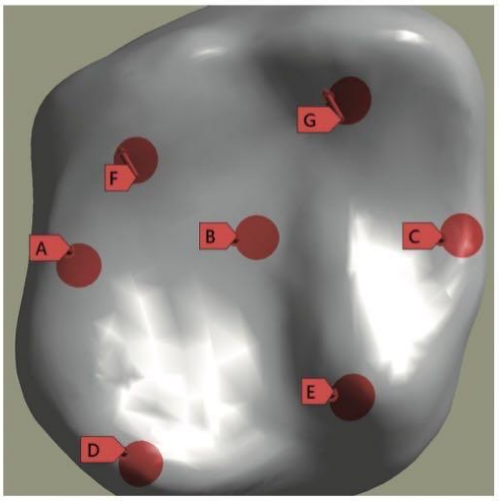

Fig. 4 Loading site.
From point A to point G, mesial limbic ridge, fossa central, distal limbic ridge, proximal palatine apex, distal palatine apex, proximal buccal apical triangular ridge, and distal buccal apical triangular ridge.

into tetrahedral entities (Fig. 3). Assuming that all components were homogeneous, linearly elastic, and isotropic, all interfaces were considered to be perfectly bonded and the bottom of the alveolar bone to be fully constrained.

The load was applied, and the index was observed. Lateral and vertical static loading modes were designed as per the study by Jiang *et al.*[21]. Additionally, the force of lateral movement was simulated by applying a 200-N oblique bite force at 45 degrees to the surface of the model and the long axis of the tooth. Vertical bite forces of 200 N and 600 N parallel to the long axis of the tooth body were applied to simulate the normal and

maximum bite forces, respectively[22,23]. Vertical loading sites included the mesial limbic ridge, central fossa, distal limbic ridge, proximal palatine apex, and distal palatine apex. The lateral loading sites were the proximal and distal buccal apical triangular cristae (Fig. 4). As tooth tissue is brittle, the observation indices selected in this experiment were the von Mises and maximum principal stresses.

RESULTS

The stress distribution of the dentin and crack defects in each group of models is shown in Figs. 5 and 6, with the red area indicating a high-stress concentration. The stress distribution at the hidden crack is closely related to the depth of the crack rather than the repair material. The maximum principal stress values are located at the bottom of the enamel side crack, indicating that the crack has a tendency to expand further toward the bottom under stress and is more prone to fracture than normal teeth. The maximum principal stress value appeared at the full-crown area when the C1 crack was completely enveloped by the full crown, demonstrating that the full-crown repair can reduce the stress intensity in the crack area and effectively delay further crack propagation. The neck crack was a stress concentration area when the end of the C2 crack was not completely enveloped by the full crown below the edge of the crown, and the maximum principal stress value was located at the enamel crack. The stress at the crack was significantly higher than that in the C1 crack. Oblique loads had a greater impact on cracks in the buccal and lingual directions than vertical loads. The maximum principal stress value of the remaining tooth tissue was mainly concentrated at the neck and fork of the palatal root when subjected to vertical forces, whereas it was primarily concentrated in the buccal direction of the root bifurcation when subjected to lateral forces.

The maximum principal stress values of the residual dentin and cryptic fissure defects in groups C1 and C2 after repair with different materials under the action of the three loads are shown in Tables 2 and 3, respectively. The von Mises stress values are listed in Tables 4 and 5. As can be seen in the tables, the maximum principal stress at the dentin crack of the two deep crack models under the same repair mode was as follows: group C2>group C1, and vertical loading 600 N>lateral loading 200 N>vertical loading 200 N, and the difference

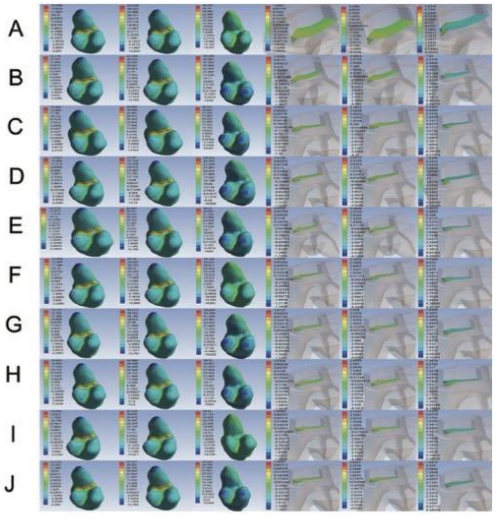

Fig. 5 Force distribution and the maximum principal stress values of each group of models in C1 (Crack 1 mm).
From A to J, they are as follows: the NP, PTP-3M, PTP-GI, PTP-ZP, GAP-3M, GAP-GI, GAP-ZP, GFP-3M, GFP-GI, and GFP-ZP groups. From left to right, a vertical load of 200 N, a vertical load of 600 N, and a lateral load of 200 N were applied to the remaining dentin and crack defects. NP, no-post; PTP, pure titanium post; GAP, gold alloy post; 3M, 3M resin; GI, glass ionomer; ZP, zinc phosphate

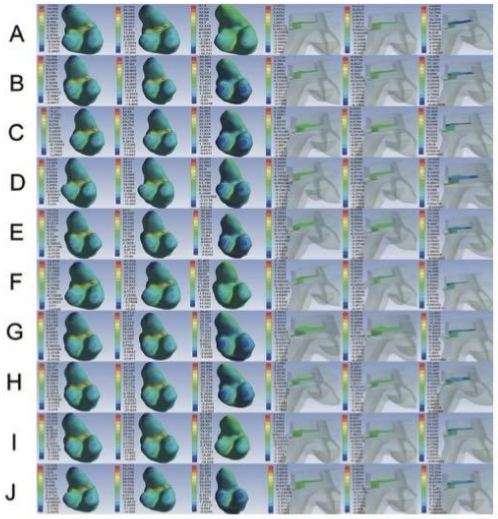

Fig. 6 Force distribution and the maximum principal stress values of each group of models in C2 (Crack 2 mm).
From A to J, they are as follows: the NP, PTP-3M, PTP-GI, PTP-ZP, GAP-3M, GAP-GI, GAP-ZP, GFP-3M, GFP-GI, and GFP-ZP groups. From left to right, a vertical load of 200 N, a vertical load of 600 N, and a lateral load of 200 N were applied to the remaining dentin and crack defects. NP, no-post; PTP, pure titanium post; GAP, gold alloy post; 3M, 3M resin; GI, glass ionomer; ZP, zinc phosphate

Table 2 Maximum principal stress values at the residual dentin and crack defects of group C1 under different loads (MPa)

Model		Residual dentin			Crack defect		
		Vertical 200 N	Vertical 600 N	Lateral 200 N	Vertical 200 N	Vertical 600 N	Lateral 200 N
NP	NP	14.486	43.458	39.375	1.053	3.160	7.235
PTP	3M	14.179	42.538	38.249	1.029	3.085	7.070
	GI	14.366	43.098	38.252	1.034	3.102	7.144
	ZP	13.957	41.870	38.245	1.010	3.031	7.031
GAP	3M	14.316	42.947	38.250	1.030	3.090	7.093
	GI	14.393	43.180	39.102	1.036	3.108	7.169
	ZP	14.172	42.517	38.246	1.013	3.038	7.050
GFP	3M	14.333	42.998	38.250	1.033	3.099	7.103
	GI	14.418	43.254	39.340	1.040	3.119	7.171
	ZP	14.176	42.527	38.246	1.021	3.062	7.068

NP, no-post; PTP, pure titanium post; GAP, gold alloy post; GFP, glass fiber post; 3M, 3M resin; GI, glass ionomer; ZP, zinc phosphate

Table 3 Maximum principal stress values at the residual dentin and crack defects of group C2 under different loads (MPa)

Model		Residual dentin			Crack defect		
		Vertical 200 N	Vertical 600 N	Lateral 200 N	Vertical 200 N	Vertical 600 N	Lateral 200 N
NP	NP	15.902	47.706	41.600	3.177	9.532	14.869
PTP	3M	15.586	46.757	40.461	3.128	9.384	13.254
	GI	15.774	47.322	40.466	3.147	9.439	13.363
	ZP	14.837	44.511	36.305	2.647	7.940	12.964
GAP	3M	15.733	47.200	40.465	3.132	9.395	13.282
	GI	15.818	47.454	41.405	3.147	9.441	13.367
	ZP	15.571	46.713	40.461	3.083	9.250	13.002
GFP	3M	15.752	47.257	40.466	3.144	9.433	13.343
	GI	15.845	47.535	41.589	3.176	9.529	13.435
	ZP	15.578	46.733	40.461	3.106	9.317	13.116

NP, no-post; PTP, pure titanium post; GAP, gold alloy post; GFP, glass fiber post; 3M, 3M resin; GI, glass ionomer; ZP, zinc phosphate

Table 4 von Mises stress value of residual dentin and hidden fissure defect in group C1 under different loads (MPa)

Model		Residual dentin			Crack defect		
		Vertical 200 N	Vertical 600 N	Lateral 200 N	Vertical 200 N	Vertical 600 N	Lateral 200 N
NP	NP	17.682	53.046	50.759	4.848	14.543	6.961
PTP	3M	17.078	51.235	31.373	4.743	14.229	6.802
	GI	17.202	51.605	31.376	4.806	14.419	6.872
	ZP	16.782	50.346	31.371	4.706	14.118	6.765
GAP	3M	17.161	51.483	31.375	4.745	14.236	6.820
	GI	17.356	52.069	31.379	4.810	14.430	6.895
	ZP	16.945	50.836	31.372	4.706	14.119	6.779
GFP	3M	17.187	51.562	31.375	4.749	14.247	6.835
	GI	17.373	52.119	31.379	4.815	14.446	6.898
	ZP	17.044	51.133	31.373	4.707	14.121	6.802

C1, crack 1 mm; NP, no-post; PTP, pure titanium post; GAP, gold alloy post; GFP, glass fiber post; 3M, 3M resin; GI, glass ionomer; ZP, zinc phosphate

Table 5 von Mises stress value of residual dentin and hidden fissure defect in group C2 under different loads (MPa)

Model		Residual dentin			Crack defect		
		Vertical 200 N	Vertical 600 N	Lateral 200 N	Vertical 200 N	Vertical 600 N	Lateral 200 N
NP	NP	17.677	53.031	52.275	10.043	30.129	11.454
PTP	3M	17.036	51.107	34.184	9.873	29.620	11.317
	GI	17.154	51.461	34.188	9.934	29.802	11.371
	ZP	16.735	50.204	28.992	9.532	28.597	10.517
GAP	3M	17.120	51.361	34.184	9.928	29.783	11.345
	GI	17.323	51.968	34.188	10.039	30.118	11.464
	ZP	16.896	50.689	28.992	9.852	29.556	11.277
GFP	3M	17.148	51.444	34.188	9.933	29.799	11.346
	GI	17.341	52.022	50.759	10.042	30.125	11.445
	ZP	17.000	51.001	34.184	9.869	29.605	11.288

C2, crack 2 mm; NP, no-post; PTP, pure titanium post; GAP, gold alloy post; GFP, glass fiber post; 3M, 3M resin; GI, glass ionomer; ZP, zinc phosphate

is obvious. Using the same post-binder, the maximum dentin principal stress values of the model groups with the same crack depth were as follows: resin-filled full crown group>fiber full crown group>gold alloy full crown group>pure titanium full crown group. Additionally, the maximum principal stress value of the residual dentin after resin-filled restoration was significantly higher than that in the three groups after post-core crown restoration. For models with the same crack depth and pile material, the maximum principal stress values of the dentin were as follows: group NP>group GI>group 3M>group ZP.

DISCUSSION

Many oral restorative materials are being used for post-core crown restorations. PTPs have stronger mechanical properties and greater hardness than non-metallic post-core materials; they can withstand greater chewing forces, produce relatively small images during the examination, and have good biocompatibility. GAPs have unique chemical stability and good mechanical properties due to their high gold content. The elastic modulus of GAPs is closer to that of dentin than that of PTPs and can absorb and redistribute stress. Fiber resin posts have good aesthetics, and their elastic modulus is comparable to that of teeth; therefore, they can effectively avoid highly concentrated stress and prevent tooth fracture. They also act as an ideal post-core crown restoration material. In addition to the post, the post binder plays an essential role in the conduction and distribution of stress when the restoration is subjected to bite force. Post-core materials with different elastic moduli exhibited different stress sizes and distributions. A binder with a low elastic modulus, such as resin, is beneficial for stress at the bond interface of the post-core crown, and its bond strength is significantly higher than that of ZP and GI cement. However, relevant studies have found that binders with high elastic moduli, such as ZP, can better buffer the stress concentration at the root canal opening, thereby avoiding tooth splitting[24].

Establishing a finite element model with high geometric similarity is difficult due to the maxillary first molars' complex morphology and root canal structure. Therefore, biomechanical studies on post-core-crown molar restorations have received little attention at home and abroad. However, with the rapid development of computer technology recently, finite element models are being established using Digital Imaging and Communications in Medicine (DICOM) data to reverse engineer technology. The use of FEA to study stress size and distribution after dental restoration has become a popular topic in the fields of dental prosthodontics and biomechanics[25,26]. A three-dimensional finite element model of molar post-core-crown restoration with high geometric similarity can be established using this modeling method, which provides conditions for stress analysis of molar post-core-crown restoration.

In this study, the scope and depth of the hidden cracks were significant factors influencing the prognosis of affected teeth, and difficulty in eliminating cracks increased the risk of treatment failure. Therefore, the existence of cracks should be fully considered before repair. Furthermore, effective repair methods should be used to increase the survival rate of the affected teeth and avoid additional treatment costs. In this experiment, two types of cracks with different depths were designed. The cracks in group C1 were located above the edge of the all-porcelain crown, and the crack end was completely hidden after being repaired by the all-porcelain crown. Group C2 cracks were located below the edge of the all-porcelain crown, and the crack ends were exposed outside the all-porcelain crown. According to the experimental results, a comparison of the stress cloud maps at the crack site under different loads revealed similar stress distribution positions for Groups C1 and C2, with the

stress concentration area and maximum principal stress value located at the end of the crack, indicating that the crack defect has a tendency to further expand under the action of force and is more prone to fracture than normal teeth. A comparison of the stress conditions of groups C1 and C2 revealed that the full crown had the best protective effect on the hidden cracks, and the stress value at the crack site was relatively small when the full crown enveloped all cracks. The von Mises and maximum principal stress values at the crack defect increase as the crack depth increases, which is consistent with previous research findings[27]. An increase in crack depth leads to an increase in the stress value at the crack tip, resulting in a decrease in the safe life of the affected tooth and the continued development of hidden cracks. Therefore, it is crucial to effectively treat teeth with hidden cracks on time to prevent the progression of cracks and achieve good long-term repair results.

In the C1 and C2 group models, as the number of loads on the residual dentin increased, the stress on it and crack defects also increased. Moreover, under the same magnitude of force, the effect of lateral loading on the residual dentin stress was greater than that of vertical loading; this finding is similar to the research results of scholars such as Martins[28]. The lateral force has a greater tensile stress on the remaining dentin, leading to a greater force for the continuous splitting of hidden cracks. This is related to the fact that the tooth tissue is a brittle material, and the compressive strength is 5–6 times the tensile strength, demonstrating the effectiveness and rationality of this model. This indicates that lateral force is the main factor causing the further development of hidden cracks.

The effects of different repair methods on the von Mises stress value and maximum principal stress peak at the crack defect were consistent at similar crack depths. The method of using resin fillings for restoration can maximize the preservation of tooth tissue and is simple to perform at reduced patient costs. However, regardless of whether it was in the C1 or C2 group, the maximum principal stress peak at the crack site in the NP group was greater than those in the PTP, GAP, and GFP groups. As the coefficient of thermal expansion of the resin material differs from that of tooth tissue, fillings with greater depth can reduce the ability of dentin to resist crack growth. Although post-core restorations remove more tooth tissue than resin-filled restorations, both fiber posts with a low elastic modulus and PTPs with a high elastic modulus can play a role in strengthening teeth. After post-core restorations, teeth can be preserved for a long time, and good long-term repair results can be achieved. Türker *et al.* found that post-core crown restoration could provide greater resistance to chewing function using FEA. Our experimental results are consistent with those of Türker *et al.*[29]. After post-core repair, the cracked maxillary first molar with defects can effectively protect the remaining tooth tissue by reducing the peak stress acting on the remaining dentin because the post bears a portion of the stress. However, the NP group had higher stress values in the dentin than the PTP, GAP, and GFP groups because of the lack of post-restoration teeth to bear stress.

These three types of pile materials have unique characteristics in clinical applications and can meet clinical needs. The von Mises and maximum principal stress distribution of the remaining dentin restored with PTP, GAP, and GFP in each group were consistent, mainly concentrated at the neck and fork of the palatal root, and were minimal when using PTP. When using the same type of post-core adhesive and GFP with a low elastic modulus, the post can effectively transfer stress to the remaining dentin, reducing post-stress, which is more beneficial for protecting the post-core restoration. When using a PTP with a high elastic modulus, the post bears more stress, and the stress transferred to the remaining dentin is relatively reduced. However, owing to the greater stress borne by the post, non-uniform and destructive forces are transmitted to the dentin, reducing the stress on the outer surface of the root and increasing the burden on the root[30]. Therefore, the existence of weak root canals should be eliminated before using PTP. In this study, the palatal root of the maxillary first molar was thick and could be repaired using PTP. It is crucial to effectively reduce the stress on the remaining dentin with hidden cracks. Thus, when repairing the maxillary first molar with hidden cracks and defects, PTP with a high elastic modulus can bear a relatively high equivalent stress, and the peak stress on the dentin will be relatively small, which can effectively slow the development of hidden cracks.

When performing post-core crown restoration, the stress protection effect of different post binders on the dental tissue greatly varies. Research has shown that when using adhesives with a higher elastic modulus, the higher the stress level of the bonding layer, the greater the impact on the stress distribution of the post-core dentin[31]. Lü *et al.* believe that high-elastic-modulus adhesives can effectively buffer the concentrated stress at the root canal opening and prevent tooth fracture; low-elastic-modulus adhesives can effectively protect the root canal, and using them is preferable for tooth tissue with thin and weak root canals[16]. In this experiment, the palatal root of the maxillary first molar was thick and did not have a weak root canal. The use of a high-elastic-modulus ZP adhesive resulted in minimal stress in the remaining dentin and crack defects, preventing further development of hidden cracks caused by stress concentration; this finding was similar to the results of previous research.

Although FEA is a widely used technology, this experiment is primarily static and does not fully simulate the functional status of the oral cavity. As in previous FEA studies, the major limitation is that many details are idealized, resulting in certain errors in the experimental results[28]. Moreover, selecting post, core, and crown repair material in clinical practice is influenced by multiple factors, and this experiment only provides a partial reference in this regard. Therefore, there is a need for further supplementation and validation of FEA-based experimental models. Additionally, the

forms of hidden cracks in teeth vary greatly, and this study only selected one representative crack form. Thus, in the future, comprehensive analysis, including other forms of cracks, is recommended.

CONCLUSIONS

Within the limitations of the FEA study, we reached the following conclusions: After post-core crown treatment of the affected teeth with cryptic fissures and defects, the therapeutic effects of repair materials differ; clinicians can specify treatment plans according to the patient's actual situation. Additionally, for the dental model in this experiment, the possibility of further propagation of hidden cracks and tooth fractures can be reduced using pure titanium metal posts with a high elastic modulus or fiber posts with a low elastic modulus and all-porcelain crown repair. The maximum principal stress at the crack and residual dentin was the lowest after repair with the pure titanium metal post, ZP binder, and porcelain crown. The lateral force ratio of the vertical force significantly influences the stress variation of the hidden crack, which easily causes propagation and fracture of the hidden crack. A deeper, hidden crack increases the likelihood of crack propagation and fracture.

CONFLICT OF INTEREST

This study did not receive any specific grants from funding agencies in the public, commercial, or non-profit sectors.

REFERENCES

1) Yu M, Li J, Liu S, Xie Z, Liu J, Liu Y. Diagnosis of cracked tooth: Clinical status and research progress. Jpn Dent Sci Rev 2022; 58: 357-364.
2) Guo J, Wu Y, Chen L, Long S, Chen D, Ouyang H, *et al.* A perspective on the diagnosis of cracked tooth: Imaging modalities evolve to AI-based analysis. Biomed Eng Online 2022; 21: 36.
3) Geurtsen W, Schwarze T, Günay H. Diagnosis, therapy, and prevention of the cracked tooth syndrome. Quintessence Int 2003; 34: 409-417.
4) Nayak A, Jain PK, Kankar PK, Jain N. Effect of volumetric shrinkage of restorative materials on tooth structure: A finite element analysis. Proc Inst Mech Eng H 2021; 235: 493-499.
5) Eram A, Zuber M, Keni LG, Kalburgi S, Naik R, Bhandary S, *et al.* Finite element analysis of immature teeth filled with MTA, Biodentine and Bioaggregate. Comput Methods Programs Biomed 2020; 190: 105356.
6) Zhu J, Rong Q, Wang X, Gao X. Influence of remaining tooth structure and restorative material type on stress distribution in endodontically treated maxillary premolars: A finite element analysis. J Prosthet Dent 2017; 117: 646-655.
7) Kim SY, Kim BS, Kim H, Cho SY. Occlusal stress distribution and remaining crack propagation of a cracked tooth treated with different materials and designs: 3D finite element analysis. Dent Mater 2021; 37: 731-740.
8) Li F, Diao Y, Wang J, Hou X, Qiao S, Kong J, *et al.* Review of cracked tooth syndrome: Etiology, diagnosis, management, and prevention. Pain Res Manag 2021; 2021: 3788660.
9) Kakka A, Gavriil D, Whitworth J. Treatment of cracked teeth: A comprehensive narrative review. Clin Exp Dent Res 2022; 8: 1218-1248.
10) de Toubes KMS, Soares CJ, Soares RV, Côrtes MIS, Tonelli SQ, Bruzinga FFB, *et al.* The correlation of crack lines and definitive restorations with the survival and success rates of cracked teeth: A long-term retrospective clinical study. J Endod 2022; 48: 190-199.
11) Eliyas S, Jalili J, Martin N. Restoration of the root canal treated tooth. Br Dent J 2015; 218: 53-62.
12) Lin J, Lin Z, Zheng Z. Effect of different restorative crown design and materials on stress distribution in endodontically treated molars: A finite element analysis study. BMC Oral Health 2020; 20: 226.
13) Yap EXY, Chan PY, Yu VSH, Lui JN. Management of cracked teeth: Perspectives of general dental practitioners and specialists. J Dent 2021; 113: 103770.
14) Oyar P. The effects of post-core and crown material and luting agents on stress distribution in tooth restorations. J Prosthet Dent 2014; 112: 211-219.
15) Verri FR, Okumura MHT, Lemos CAA, Almeida DAF, de Souza Batista VE, Cruz RS, *et al.* Three-dimensional finite element analysis of glass fiber and cast metal posts with different alloys for reconstruction of teeth without ferrule. J Med Eng Technol 2017; 41: 644-651.
16) Lü LW, Meng GW, Liu ZH. Finite element analysis of multi-piece post-crown restoration using different types of adhesives. Int J Oral Sci 2013; 5: 162-166.
17) Li X, Kang T, Zhan D, Xie J, Guo L. Biomechanical behavior of endocrowns vs fiber post-core-crown vs cast post-core-crown for the restoration of maxillary central incisors with 1 mm and 2 mm ferrule height: A 3D static linear finite element analysis. Medicine (Baltimore) 2020; 99: e22648.
18) Lee JH, Jang HY, Lee SY. Finite element analysis of dental implants with zirconia crown restorations: Conventional cement-retained vs. cementless screw-retained. Materials (Basel) 2021; 14: 2666.
19) Savychuk A, Manda M, Galanis C, Provatidis C, Koidis P. Stress generation in mandibular anterior teeth restored with different types of post-and-core at various levels of ferrule. J Prosthet Dent 2018; 119: 965-974.
20) Wimmer T, Erdelt KJ, Raith S, Schneider JM, Stawarczyk B, Beuer F. Effects of differing thickness and mechanical properties of cement on the stress levels and distributions in a three-unit zirconia fixed prosthesis by FEA. J Prosthodont 2014; 23: 358-366.
21) Jiang Q, Huang Y, Tu X, Li Z, He Y, Yang X. Biomechanical properties of first maxillary molars with different endodontic cavities: A finite element analysis. J Endod 2018; 44: 1283-1288.
22) Mahrous A, Alagha E, Almutairi T, Albishi F, Alfayomi I, Rasheed N. Finite element analysis of restored principal abutment in free-end saddle partial denture. Clin Cosmet Investig Dent 2022; 14: 11-17.
23) Eshghpour M, Samieirad S, Shooshtari Z, Shams A, Ghadirimoghaddam N. Three different fixation modalities following mandibular setback surgery with sagittal split ramus osteotomy: A comparative study using three-dimensional finite elements analysis. World J Plast Surg 2023; 12: 43-57.
24) Li LL, Wang ZY, Bai ZC, Mao Y, Gao B, Xin HT, *et al.* Three-dimensional finite element analysis of weakened roots restored with different cements in combination with titanium alloy posts. Chin Med J (Engl) 2006; 119: 305-311.
25) Yamaguchi S, Katsumoto Y, Hayashi K, Aoki M, Kunikata M, Nakase Y, *et al.* Fracture origin and crack propagation of CAD/CAM composite crowns by combining of in vitro and in silico approaches. J Mech Behav Biomed Mater 2020; 112: 104083.
26) Hoshino IAE, Dos Santos PH, Briso ALF, Sundfeld RH, Yamaguchi S, Rocha EP, *et al.* Biomechanical performance

of three fiberglass post cementation techniques: Imaging, in vitro, and in silico analysis. J Prosthodont Res 2023; 67: 103-111.
27) Hou TZ, Zhu FY, Tao H, Wang SS. Three-dimensional finite element analysis of the change of cracks in the cracked first mandibular molar under different loading conditions. Hua Xi Kou Qiang Yi Xue Za Zhi 2009; 27: 126-129.
28) Martins LM, de Lima LM, da Silva LM, Cohen-Carneiro F, Noritomi PY, Lorenzoni FC. Crown materials and the occlusal thickness affect the load stress dissipation on 3D molar crowns: Finite element analysis. Int J Prosthodont 2023; 36: 301-307.
29) Türker SA, Özçelik B, Yilmaz Z. Evaluation of the bond strength and fracture resistance of different post systems. J Contemp Dent Pract 2015; 16: 788-793.
30) Nahar R, Mishra SK, Chowdhary R. Evaluation of stress distribution in an endodontically treated tooth restored with four different post systems and two different crowns —A finite element analysis. J Oral Biol Craniofac Res 2020; 10: 719-726.
31) Spazzin AO, Galafassi D, de Meira-Júnior AD, Braz R, Garbin CA. Influence of post and resin cement on stress distribution of maxillary central incisors restored with direct resin composite. Oper Dent 2009; 34: 223-229.